Microchemical Journal 212 (2025) 113176

Contents lists available at ScienceDirect

Microchemical Journal

journal homepage: www.elsevier.com/locate/microc

An aptamer/CRISPR electrochemical (ACE) biosensor for *Plasmodium falciparum* histidine-rich protein II and SARS-CoV-2 nucleocapsid protein

Young Lo [a,1], Ryan H.P. Siu [a,1], Chau Tran [a], Robert G. Jesky [a], Andrew B. Kinghorn [a], Julian A. Tanner [a,b,c,*]

[a] School of Biomedical Sciences, LKS Faculty of Medicine, The University of Hong Kong, PR China
[b] Advanced Biomedical Instrumentation Centre, Hong Kong Science Park, PR China
[c] Materials Innovation Institute for Life Sciences and Energy (MILES), HKU-SIRI, Shenzhen, PR China

ARTICLE INFO

Keywords:
CRISPR
Electrochemical Aptamer biosensor
Malaria
Plasmodium falciparum histidine-rich protein II
SARS-CoV-2 nucleocapsid protein

ABSTRACT

The *trans*-cleavage activity of CRISPR Cas12 and Cas13 on single-stranded DNA has been widely applied for biosensing and diagnostic applications. Typically, such approaches have traditionally been limited to the sensing of nucleic acids. Here, we have combined CRISPR Cas12 with nucleic acid aptamers to enable protein recognition by an electrochemical approach. To demonstrate the versatility of this approach, we have successfully detected two important protein disease biomarkers: *Plasmodium falciparum* histidine-rich protein II (*PfHRP2)* as a biomarker of malaria, and SARS-CoV-2 nucleocapsid (N) protein as a biomarker of COVID. We designed activable aptasensors by annealing aptamers to a complementary locking strand. CRISPR Cas12 *trans*-cleavage is initiated by strand displacement upon protein binding, thereby cleaving a redox reporter conjugated to DNA on an electrode, transducing into an electrochemical signal. The limits of detection for *PfHRP2* and COVID N protein are 45.5 nM and 8.18 nM respectively with high specificity towards their targets. Protein detection by such CRISPR-assisted ACE biosensors can be potentially expanded and multiplexed across several critical biomarkers in parallel.

1. Introduction

Clustered Regularly Interspaced Short Palindromic Repeats (CRISPR)-associated enzymes derive from the adaptive immune systems of bacteria and archaea. These enzymes use RNA-guided nucleases (gRNA/crRNA) to recognize and degrade foreign nucleic acids [1,2]. Since the discovery and characterization of the first CRISPR enzyme, CRISPR/Cas9, CRISPR/Cas systems have attracted increasing attention [3]. Primarily seen as a powerful gene editing tool [4,5], the CRISPR toolbox is rapidly expanding into diagnostics and biosensing by exploiting the collateral DNase activity [6]. CRISPR/Cas12a, previously known as CpfI, is a Class 2 type V CRISPR/Cas effector that cleaves target DNA guided by a crRNA (CRISPR RNA). Unlike Cas9, Cas12a possesses target-dependent non-specific single-stranded DNA (ssDNA) DNAse activity, termed "*trans*-cleavage" [6–8].

Cas12a catalyzes the degradation of random ssDNA in the presence of a crRNA and its complementary target ssDNA, often termed as the activator [6]. By this mechanism, the Cas12a-crRNA complex in the presence of the activator ssDNA performs robust, non-specific ssDNA *trans*-cleavage activity. This activity has been utilized in sensing applications. Prof. Doudna and her colleagues created the DNA Endonuclease-Targeted CRISPR Trans Reporter (DETECTR) for ultra-sensitive detection of human papillomavirus (HPV). DETECTR used the *Lachnospiraceae bacterium* (Lb) Cas12a with a fluorophore quencher (FQ)-labeled ssDNA reporter system, and has been demonstrated in the clinical environment [6]. CRISPR-based biosensors operating by similar mechanisms have been widely reported to detect various nucleic acid targets including SARS-CoV-2 [9–12], HPV [13], HBV [14], HIV [15], influenza virus [16], dengue virus [17], Ebola virus [18], pathogenic bacteria [19] and other diseases.

Beyond nucleic acid testing, CRISPR approaches have been rapidly expanded to detect non-nucleic acid targets [20]. These includes metal ions and small molecules contamination in environmental and food safety research [21–26], as well as pathogenic proteins biomarkers and tumor cells detection in clinical settings [27–29]. This flexibility is largely conferred by the integration of nucleic acid aptamers which can

* Corresponding author.
E-mail address: jatanner@hku.hk (J.A. Tanner).
[1] These authors contributed equally to this work.

https://doi.org/10.1016/j.microc.2025.113176
Received 15 August 2024; Received in revised form 12 December 2024; Accepted 25 February 2025
Available online 26 February 2025

bind to a wide range of targets. Typically, aptamer-mediated target recognition activates a *trans*-cleavage reaction generating a measurable signal. Fluorescence readout has been the primary signal transduction mechanism using a pair of fluorophore and quencher cleaved by the activated Cas enzyme [30,31]. Limited studies have expanded the application to other sensing platforms [32–34]. One of the latest applications of CRISPR is electrochemical sensing which offers advantages including cost-effectiveness, rapid testing and easily miniaturizable, which is ideal for Point of Care Testing (POCT) [19,35–37].

Herein, we have developed the Aptamer/CRISPR Electrochemical (ACE) sensor to detect two important biomarkers – *PfHRP2* for malaria diagnosis, and SARS-CoV-2 nucleocapsid (N) protein for COVID-19 diagnosis. Unlike the first-generation fluorescence readouts such as the DETECTR and Specific High-sensitivity Enzymatic Reporter Unlocking (SHERLOCK), the ACE sensor converts the collateral cleavage activity into electrochemical signals. Specifically, trans cleavage on the electrode immobilized with redox reporter conjugated ssDNA substrates substantially reduces the surface reporter density and amplifies the detection signal. In addition, our proposed ACE sensor focuses on customizing a ssDNA locked activator complementary to the aptamer sequence to silence the trans cleavage activity, thereby avoiding off-target responses when the target protein is absent. We optimize the design of the activator strands to enable strand displacement from protein binding and subsequent crRNA hybridization to activate the Cas enzyme. We describe the optimization of lock activators and the electrochemical assay to provide evidence of feasibility in detecting both *PfHRP2* and N protein using this model.

Furthermore, the proposed ACE biosensor offers comparative advantages over traditional protein detection methodologies such as proximity ligation assay, which often has size restrictions for the target protein (<40 nm) and requires a pair of sandwich antibodies recognizing the target [38,39]. Through customizing a single-stranded DNA locked activator complementary to the aptamer identified for a specific protein target, the scope of detection by our ACE biosensor can be expanded across critical protein biomarkers.

2. Experimental

2.1. Materials and Instruments

All oligonucleotides were ordered from Integrated DNA Technologies (Coralville, US). PolyA oligonucleotides with methylene blue (MB) and thiol modification and crRNA sequences were purified by HPLC. The sequences of aptamers, ssDNA locked activators, crRNA and polyA substrate strand were summarized in Table S1. All malaria protein biomarkers were expressed in-house using *Escherichia coli*. SARS-CoV-2 nucleocapsid protein was purchased from SinoBiological (China). EnGen® Lba Cas12a was purchased from New England Biolabs (UK). SYBR gold nucleic acid stain was purchased from Invitrogen. SUPERase•In™ RNase Inhibitor was purchased from ThermoFisher Scientific. All other chemicals were obtained from Sigma Aldrich.

All electrochemical measurements were conducted using PalmSens4 potentiostat purchased from PalmSens (Houten, Netherlands). Gold rod electrodes, platinum counter electrodes, and silver/silver chloride reference electrodes were also purchased from PalmSens.

2.2. Aptamer lock duplex assembly

Aptamer duplexes consisted of aptamer with complementary activator DNA (1:1 M ratio) were annealed in hybridization buffer (10 mM Tris HCl, pH 8.0, 100 mM NaCl and 1 mM EDTA). A thermal cycler was used to incubate at 95 °C for 5 min followed by cooling at a steady rate of 1 °C per min until 20 °C was reached. Aptamer duplexes were characterized by native 10 % Polyacrylamide Gel Electrophoresis (PAGE) run in 1x TBE buffer.

2.3. Electrophoretic mobility shift assay (EMSA)

For testing the strand displacement efficiency by *PfHRP2*, the constructed 2106s aptamer duplexes (100 nM) were incubated with 2 μM protein at 25 °C for 1 h. Protein-bound aptamers were resolved from the activator duplex on a TBE discontinuous native PAGE consisted of 6 % stacking gel and 12 % resolving gel. The gels were stained using SYBR gold nucleic acid stain (ThermoFisher Scientific) before imaging using ChemiDoc™ Touch Gel Imaging System (Bio-Rad).

2.4. Plate binding assay

For testing the strand displacement efficiency by SARS-CoV-2 N protein, recombinant His-tagged protein was coated onto Pierce™ Nickel Coated Plates (ThermoFisher Scientific) with shaking at 4°C. The plate wells were then washed with PBST (0.05 % Tween 20) 3 times. Then 5 % BSA was applied to block the wells followed by washing with PBST three times. 100 μl of 50 nM aptamer A58 or aptamer/activator duplexes were then incubated for 1 h in RT with shaking to allow binding and release of the activator complementary strand. The plate was then carefully washed four times with PBST. The aptamer strands were eluted in 1 % sodium dodecyl sulfate (SDS) solution and analyzed by SYBR Gold stained 10 % native PAGE.

2.5. Electrode fabrication and functionalization

Preparation of the working electrode for aptamer immobilization started with polishing the probe gold surface sequentially in 1 μm and 0.03 μm aluminum oxide powder on a microcloth surface for 1 min each. The polished electrodes were then sonicated for 5 mins in distilled water to remove any remaining polishing agents. Further cleaning of the electrode via cyclic voltammetry scanning under basic conditions (0.5 M NaOH) over the potential range −0.35 to −1.35 V was performed. Followed by scans under acidic conditions (0.5 M H_2SO_4) over the potential 0 to 1.5 V. Final scans under acidic 0.01 M KCl/0.1 M H_2SO_4 solution were performed at four different potential ranges: (1) from 0.2 to 0.75 V; (2) from 0.2 to 1 V; (3) from 0.2 V to 1.25 V; (4) from 0.2 V to 1.5 V. After, 20nt polyA oligo modified with MB and thiol group was pre-treated with TCEP (the molar ratio of oligo to TCEP was 1:100) for 2 h at room temperature (RT) to cleave the disulfide bond. Then, 250 μl of the pre-treated oligo (300 nM) was immobilized onto the surface of prepared interrogating electrodes for 2 h in a sealed, dark RT condition. After immobilization, the electrodes were rinsed with MilliQ water and the blank sites were blocked with 400 μl of 2 mM 6-mercapto-1-hexanol (MCH) in a sealed, dark RT condition overnight. Any unbound MCH was thoroughly washed away with MilliQ water. The resulting MB-oligo immobilized biosensor was stored in PBS at 4 °C before use.

2.6. CRISPR Cas12a trans-cleavage

The Cas12a-crRNA duplex (1:1 M ratio) was prepared in a buffer with nuclease free water containing 50 mM NaCl, 10 mM Tris-HCl, 15 mM $MgCl_2$, 100 μg/ml BSA, 1 % (v/v) RNAse inhibitor with a pH of 7.9. Cas12a-crRNA was assembled and incubated at 25 °C for 10 min prior to detection. For protein detection, a total volume of 150 μl of aptamer-locked activator duplex was incubated with target protein at room temperature for 60 min to allow duplex release. A 1:1 ratio of duplex-sample to Cas12a-crRNA (150 μl of duplex-sample added to 150 μl of the Cas12a-crRNA duplex) was used to form the Cas12a-crRNA-open activator triplex. After 10 mins, the interrogating electrode, with immobilized 20 nucleotide-MB, was placed with the Cas12a-crRNA-open activator triplex at 37 °C for *trans*-cleavage activity for 30 min. following this, the enzymatic reaction was stopped by washing the electrode in PBS for 5 min, and the MB signal was measured by Square Wave Voltammetry (SWV).

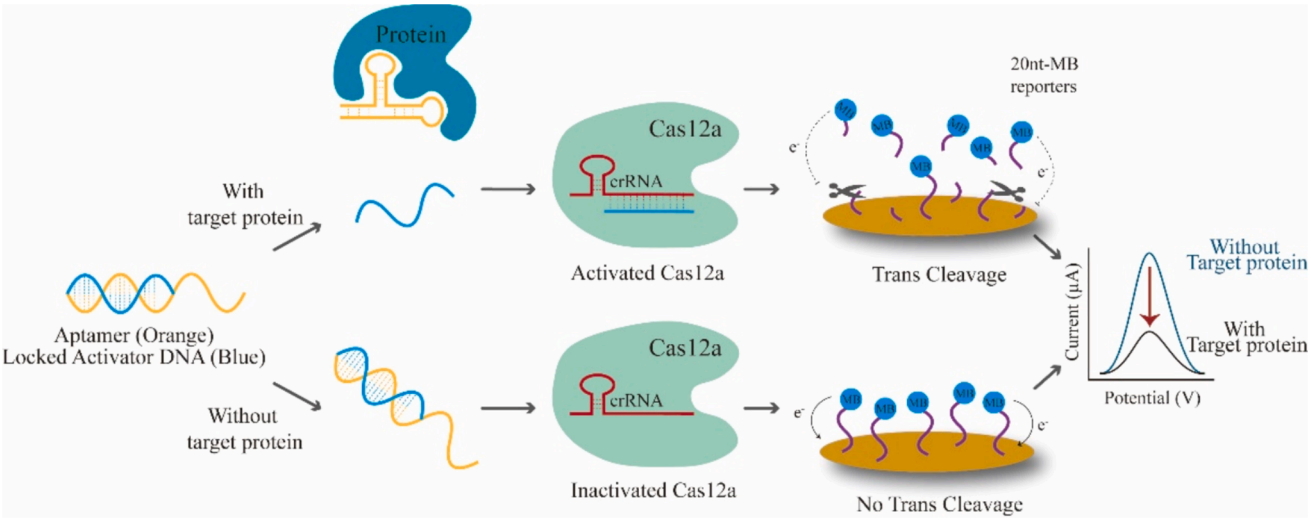

Fig. 1. Design of the Aptamer/CRISPR Electrochemical (ACE) biosensor. The locked aptasensor undergoes strand displacement upon target protein binding. The displaced activator then binds the Cas12/crRNA complex to activate *trans*-cleavage activity. The electrode bound MB poly-A reporter is cleaved and dissipates, decreasing the oxidative current intensity on the electrode.

2.7. Electrochemical measurement

Electrochemical experiments were performed with a three-electrode system consisting of: the assembled MB-DNA immobilized gold surface rod interrogating electrode, the platinum wire counter electrode, and silver/silver chloride (3 M KCl) reference electrode. SWV was carried out in 1X PBS with the potential range of −0.5 to 0 V, an amplitude of 25 mV, step size of 2 mV and frequency at 25 Hz. Measurements were conducted before and after treating the modified electrodes with the activated CRISPR Cas12a complex. Signal change was calculated as percentage decrease of the SWV peak signal after treatment. All statistical analysis (Student's *t* test) and plots were generated using Origin.

3. Results and Discussion

3.1. Design and principle of the Aptamer/CRISPR electrochemical (ACE) sensor

The ACE sensor consists of a probe system containing the target specific aptamer hybridized to a DNA activator designed for LbCas12a and a reporter system containing a pre-assembled 20nt Poly(A) oligonucleotide with an MB redox reporter immobilized onto an interrogated gold electrode (Fig. 1). MB-Poly(A) sequence was applied as the reporter because Cas12 is known to exhibit *trans*-cleavage activity towards linear ssDNA reporter while secondary structure such as G quadruplexes can diminish the enzymatic efficiency [40,41]. The electron transfer kinetics from MB are monitored by a forward potential scanning (towards positive potential against reference electrode) square wave voltammetry (SWV) using a portable potentiostat. The aptamers employed in this study are aptamer 2106s, which binds to malaria *PfHRP2* [42] and aptamer A58, which binds to SARS-CoV-2 N protein [43].

In the absence of the protein target, the aptamer (orange) binds tightly to the DNA activator (blue) with a melting temperature above ambient temperature. This prevents the activator from binding to the Cas12a-crRNA complex. However, in the presence of the target protein, aptamer is released from the DNA hybrid and preferentially binds to their target because the affinity of aptamer-protein interaction is stronger than the partial hybridization between the activator DNA and the aptamer. The released DNA activator can then hybridize with the Cas12a-associated crRNA (red). This triggers Cas12a *trans*-cleavage activity, resulting in the cleavage of the ssDNA-MB reporter (purple) off the electrode surface. The change in MB signal can be measured by the forward potential scanning SWV. The magnitude of signal reduction is directly related to the concentration of the target.

3.2. Optimization of locked activator system for PfHRP2

The optimal activator DNA length was predicted based on Mfold predictive binding regions of the *PfHRP2* aptamer (Fig. S1a). DNA activator lengths between 11 and 21 bases, covering segments of the binding region, were investigated. It was found that the minimal length of activator DNA was 12 bp whereas 8 bp locking activator failed to form a stable duplex (Fig. S2).

EMSA was used to verify Mfold predictions and observe the extent of strand displacement in the absence and presence of *PfHRP2* at different lengths of duplex pairs. The protein can displace aptamer-activator duplexes of 24 bp, 20 bp, 16 bp and 12 bp (Fig. S2). However, the aptamer binding region is between bases 10 and 22 so we decided to further characterize the strand displacement efficiency of 16 bp and 20 bp duplex based on the electrochemical assay described later.

The probe density on the electrode was then optimized. A high probe density increases molecular crowding, and the degree of available cleavage may not be sufficient for a quality signal. Alternatively, low probe density may lead to low MB baseline signals. Therefore, a titration of ssDNA-MB redox reporter was performed to determine the optimal packing density to signal change ratio. It was found that 300 nM of 20nt-MB showed the highest signal change upon *trans*-cleavage activation (Fig. S3). At this particular reporter density, the signal of MB remained stable over 14 days of storage in 4°C with less than 5 % signal loss (Fig. S4).

Based on the studies done by Dai, Zhang and Doudna, LbCas12a's RuvC catalytic domain cleaves ssDNA through a two-metal ion mechanism in which the Mg^{2+} ions are a key factor [6,41,44]. We therefore evaluated the optimal concentration of Mg^{2+} ions for *trans*-cleavage activity in our *in vitro* assay. We observed that reaction buffer containing 15 mM $MgCl_2$ resulted in the highest signal change after 60 mins which is consistent with previous studies [44] (Fig. S5).

3.3. Optimization of the activatable ACE sensor for PfHRP2

With our optimized buffer conditions and probe density, subsequent experiments were carried out with the aptamer-locked activator duplex. Significant signal change was only observed when all components (LbCas12a-crRNA, activator DNA, and target *PfHRP2)* were present

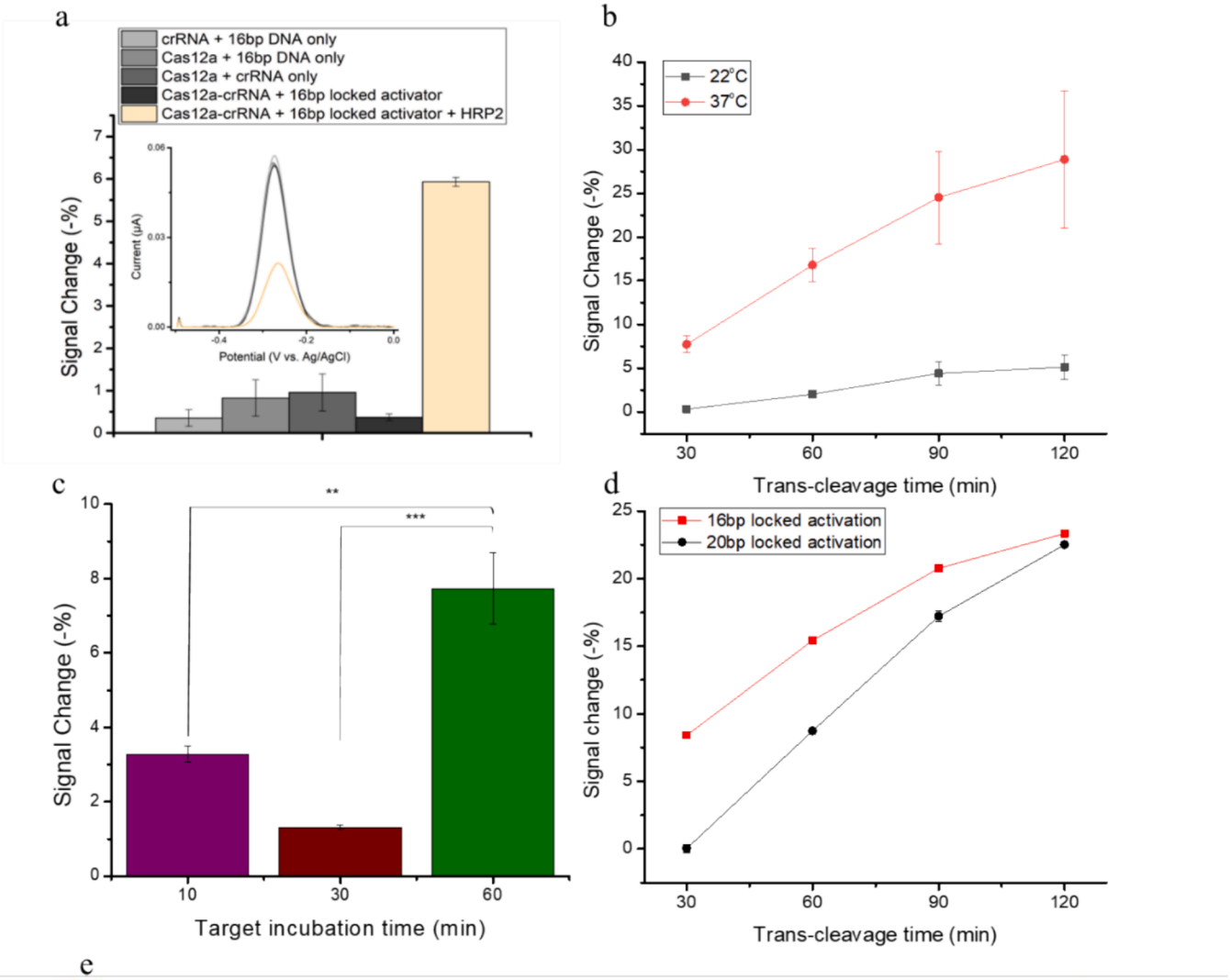

e

Conditions tested	Optimal condition
Temperature (℃): 22, 37	37 ℃
Trans-cleavage time (min): 30, 60, 90, 120	30 min
Locked duplex + target protein incubation (min): 10, 30, 60	60 min
Locked activator length (bp): 16, 20	16 bp

Fig. 2. Optimization of the ACE sensor system for *PfHRP2*. (a) Component control experiments (b) Trans-cleavage activity comparison on temperature (22 °C and 37 °C) and cleavage time-course (30 to 120 min). (c) Trans-cleavage activity comparison on target binding time-course (10, 30 and 60 min) using the 16nt activator DNA. (d) Trans-cleavage activity comparison of aptamer duplex length (16 and 20 bp) (e) Summary of optimized condition for *PfHRP2* sensing. All measurements were conducted in triplicate (three individual electrodes) and the signal change was calculated as the difference in methylene blue redox signal before and after the *trans*-cleavage reaction under the given conditions. (For interpretation of the references to colour in this figure legend, the reader is referred to the web version of this article.)

(Fig. 2a). Several negative controls were used, and in all cases, no signal was observed when any component was missing (Fig. 2a). The signal increased with time from 30 min to 2 h *trans*-cleavage incubation and a minimum of 30 min was sufficient to generate significantly higher signal change at 37 °C than at 25 °C (Fig. 2b) ($p = 0.0002$). Thus, we chose 30 min incubation at 37 °C for *trans*-cleavage activity to minimize assay time.

We next investigated the time for effective displacement of the locked activator by *PfHRP2* aptamer binding. Time points of 10, 30, and 60 min of incubation of target *PfHRP2* against 2106s-locked activator duplex at room temperature were tested. It was found that 60 min was the minimum time required for the 2106s aptamer to bind to *PfHRP2* and release the 16nt activator DNA (Fig. 2c). A shorter DNA activator length, such as 12 bp, may have increased the displacement efficiency, however such a short length may contribute to an unstable duplex structure or background displacement. When comparing 16 bp and 20 bp locked activator duplexes, they both reached similar levels of signal change after 120 min of *trans*-cleavage activation (Fig. 2d). As the 16 bp

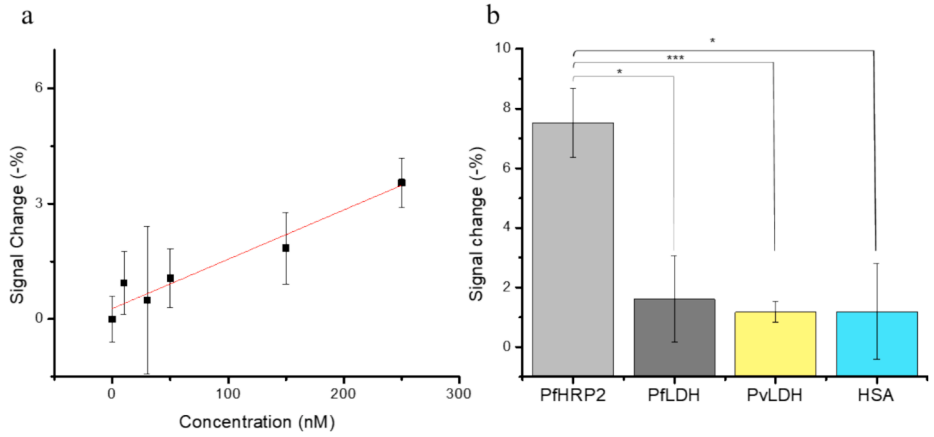

Fig. 3. (a) Linear concentration response of *PfHRP2* ACE biosensor. The calibration plot was based on the relative change of the methylene blue peak signal before and after the Aptamer/CRISPR *trans*-cleavage reaction normalized to blank (0 nM *PfHRP2*). (b) Specificity of *PfHRP2* biosensor. N = 3 for each condition. (For interpretation of the references to colour in this figure legend, the reader is referred to the web version of this article.)

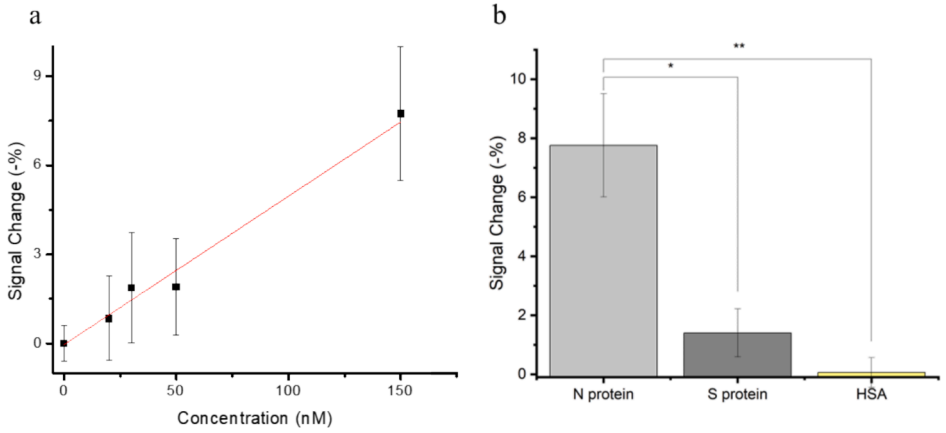

Fig. 4. (a) Linear concentration response of N protein in the ACE biosensor. The calibration plot was based on the relative change of the methylene blue peak signal before and after the Aptamer/CRISPR *trans*-cleavage reaction normalized to blank (0nM N protein). (b) Specificity of N protein biosensor. N = 3 for each condition. (For interpretation of the references to colour in this figure legend, the reader is referred to the web version of this article.)

length allowed for a quicker displacement by *PfHRP2*, it yielded a significantly higher signal change within 30 min compared to the 20 bp length ($p < 0.0001$). The 16 bp locked activator and optimized conditions (Fig. 2e) were used for the subsequent detection experiments.

3.4. Sensitivity and specificity of the 2106 s-16 bp ACE sensor

Under the optimized conditions, we assessed the sensitivity of the *PfHRP2* ACE sensing prototype in PBS. As shown in Fig. 3a, the *PfHRP2* biosensor detects the biomarker with a linear range from 10 to 250 nM. The calculated limit of detection (LOD) is 45.5 nM based on 3*(σ/Slope) model. According to the literature, patient plasma exhibits a wide concentration range of *PfHRP2* from 4 pM to 250 nM with a median of 15 nM [45]. The sensitivity of the CRISPR biosensor falls within this range, indicating its feasibility for clinical application.

The 2106s aptamer integrated ACE is highly selective to the target biomarker. The ACE sensor exhibited significantly higher signal change when incubated with target *PfHRP2* whereas non-target proteins such as *PfLDH* ($p = 0.0053$), *PvLDH* ($p = 0.0008$) and HSA ($p = 0.0052$) all failed to initiate effective *trans*-cleavage activity (Fig. 3b).

3.5. Detection of SARS-CoV-2 nucleocapsid protein by the ACE biosensor approach

To show our system's flexibility, we demonstrated the detection of SARS-CoV-2 N protein detection using our ACE biosensor approach. We employed the aptamer A58, previously shown to bind to the N protein [43], to design the specific locking strand. From the gel result shown in Fig. S6, complementary strands shorter than 14nt failed to form a stable aptamer-activator duplex. Therefore, we determined the minimal duplex length is 14 bp. Next, we verified the optimal duplex length based on strand displacement efficiency. We performed the 96-well plate binding assay and ran the eluted captured single-stranded aptamer on a gel. The native PAGE showed that strand displacement occurred only for 14 bp duplex (Fig. S7). This correlated to the predicted MFold structure (Fig. S1b) in which a longer locking strand linearizes the loop structure responsible for protein recognition via complementary base pairing. The longer locking strands reduced the aptamer binding affinity, inhibiting strand displacement and capturing of single-stranded aptamer by target protein. We therefore determined the optimal duplex length for aptamer A58 to be 14 bp.

Using the optimized 14nt activator and the ACE detection parameters optimized for *PfHRP2* with minor modifications to the SARS-CoV-2 N protein detection, specific detection of N protein relative to control non-target S protein ($p = 0.0047$) and HSA ($p = 0.0024$) was achieved (Fig. 4b). A linear detection range was observed from 20 to 150 nM of N protein in PBS (Fig. 4a). The estimated LOD of the N protein ACE sensor is 8.18 nM. This detection limit falls within the higher end of N protein concentration range in nasopharyngeal swab sample where the estimated Ct value is around 15 [46]. Further experiments will optimize

ACE detection parameters and will integrate alternative signal amplification methods to improve sensitivity.

4. Conclusions

Herein, we have demonstrated an Aptamer/CRISPR Electrochemical (ACE) sensor capable to detect both malaria *PfHRP2* and SARS-CoV-2 nucleocapsid protein. The lock-and-key aptamer mediated detection strategy is a novel approach for protein detection in CRISPR Cas-based assays. By optimizing the lock activator based on the predicted aptamer secondary structure, this target-responsive aptamer-activator strategy successfully eliminates the potential off-target initiated *trans*-cleavage signal while reaching sensitivity within a clinically relevant range. To achieve a lower protein detection range for early diagnosis, future studies could improve sensitivity through crRNA engineering [47]. The versatility of the assay, combined with the advantages of electrochemical signaling, opens opportunities for developing universal and ultrasensitive CRISPR based protein biosensors for disease diagnosis in POCT settings.

CRediT authorship contribution statement

Young Lo: Writing – original draft, Visualization, Methodology, Investigation, Formal analysis, Conceptualization. **Ryan H.P. Siu:** Writing – original draft, Visualization, Methodology, Investigation, Formal analysis, Data curation. **Chau Tran:** Methodology, Conceptualization. **Robert G. Jesky:** Methodology, Conceptualization. **Andrew B. Kinghorn:** Writing – review & editing. **Julian A. Tanner:** Writing – review & editing, Supervision, Project administration, Funding acquisition.

Declaration of competing interest

The authors declare that they have no known competing financial interests or personal relationships that could have appeared to influence the work reported in this paper.

Acknowledgements

This work was supported by HKU Seed Funding for Translational and Applied Research 2020/21 “Digital Diagnostics Using CRISPR-Enabled Nucleic Acid Probe Platform” and by HKU Seed Funding for Translational and Applied Research 2023/24 “Development of an organic electrochemical transistor-based electrochemical aptamer biosensor”. The work was also supported by Innovation and Technology Commission Public Sector Trial Scheme for the Prevention and Control of COVID-19 in Hong Kong “COVID-19 Point-of-Care Diagnostics in Saliva: an Aptamer-Mediated Approach” Project Code SST/118/20GP. This work was also supported by the Health@InnoHK program of the Innovation and Technology Commission of the Hong Kong SAR Government.

Appendix A. Supplementary data

Supplementary data to this article can be found online at https://doi.org/10.1016/j.microc.2025.113176.

Data availability

Data will be made available on request.

References

[1] R. Barrangou, *The roles of CRISPR–Cas systems in adaptive immunity and beyond*, Curr. Opin. Immunol. 32 (2015) 36–41.
[2] F. Hille, H. Richter, S.P. Wong, M. Bratovič, S. Ressel, E. Charpentier, *The Biology of CRISPR-Cas: Backward and Forward*, Cell 172 (6) (2018) 1239–1259.
[3] M. Redman, A. King, C. Watson, D. King, *What is CRISPR/Cas9?* Archives of disease in childhood, Education and Practice Edition 101 (4) (2016) 213–215.
[4] P.D. Hsu, E.S. Lander, F. Zhang, *Development and applications of CRISPR-Cas9 for genome engineering*, Cell 157 (6) (2014) 1262–1278.
[5] F. Zhang, Y. Wen, X. Guo, *CRISPR/Cas9 for genome editing: progress, implications and challenges*, Hum. Mol. Genet. 23 (R1) (2014) R40–R46.
[6] J.S. Chen, E. Ma, L.B. Harrington, M. Da Costa, X. Tian, J.M. Palefsky, J.A. Doudna, *CRISPR-Cas12a target binding unleashes indiscriminate single-stranded DNase activity*, Science 360 (6387) (2018) 436–439.
[7] S. Stella, P. Mesa, J. Thomsen, B. Paul, P. Alcon, S.B. Jensen, M.E. Moses, G. Montoya, N.S. Hatzakis, *Direct Observation of CRISPR-Cas12 Conformational Sampling by SM FRET and Cryo EM Reveals how Conformational Activation Promotes Catalysis and Resetting of the Endonuclease Activity*, Biophys. J . 118 (3) (2020) 223a–a224.
[8] B. Zetsche, J.S. Gootenberg, O.O. Abudayyeh, I.M. Slaymaker, K.S. Makarova, P. Essletzbichler, S.E. Volz, J. Joung, J. Van Der Oost, A. Regev, *Cpf1 is a single RNA-guided endonuclease of a class 2 CRISPR-Cas system*, Cell 163 (3) (2015) 759–771.
[9] J.P. Broughton, X. Deng, G. Yu, C.L. Fasching, V. Servellita, J. Singh, X. Miao, J. A. Streithorst, A. Granados, A. Sotomayor-Gonzalez, *CRISPR–Cas12-based detection of SARS-CoV-2*, Nat. Biotechnol. 38 (7) (2020) 870–874.
[10] Y. Liang, H. Lin, L. Zou, X. Deng, S. Tang, *Rapid detection and tracking of Omicron variant of SARS-CoV-2 using CRISPR-Cas12a-based assay*, Biosens. Bioelectron. (2022) 114098.
[11] C.S. Talwar, K.-H. Park, W.-C. Ahn, Y.-S. Kim, O.S. Kwon, D. Yong, T. Kang, E. Woo, *Detection of Infectious Viruses Using CRISPR-Cas12-Based Assay*, Biosensors 11 (9) (2021) 301.
[12] Z. Ali, R. Aman, A. Mahas, G.S. Rao, M. Tehseen, T. Marsic, R. Salunke, A. K. Subudhi, S.M. Hala, S.M. Hamdan, *iSCAN: An RT-LAMP-coupled CRISPR-Cas12 module for rapid, sensitive detection of SARS-CoV-2*, Virus Res. 288 (2020) 198129.
[13] L. Jubair, S. Fallaha, N.A. McMillan, *Systemic delivery of CRISPR/Cas9 targeting HPV oncogenes is effective at eliminating established tumors*, Mol. Ther. 27 (12) (2019) 2091–2099.
[14] R. Ding, J. Long, M. Yuan, X. Zheng, Y. Shen, Y. Jin, H. Yang, H. Li, S. Chen, G. Duan, *CRISPR/Cas12-Based ultra-sensitive and specific point-of-care detection of HBV*, Int. J. Mol. Sci. 22 (9) (2021) 4842.
[15] R. Nouri, Y. Jiang, X.L. Lian, W. Guan, *Sequence-specific recognition of HIV-1 DNA with solid-state CRISPR-Cas12a-assisted nanopores (SCAN)*, ACS Sensors 5 (5) (2020) 1273–1280.
[16] B.J. Park, M.S. Park, J.M. Lee, Y.J. Song, *Specific detection of influenza A and B viruses by CRISPR-Cas12a-based assay*, Biosensors 11 (3) (2021) 88.
[17] H. Li, S. Wang, X. Dong, Q. Li, M. Li, J. Li, Y. Guo, X. Jin, Y. Zhou, H. Song, *CRISPR-Cas13a cleavage of dengue virus NS3 gene efficiently inhibits viral replication*, Molecular Therapy-Nucleic Acids 19 (2020) 1460–1469.
[18] P. Qin, M. Park, K.J. Alfson, M. Tamhankar, R. Carrion, J.L. Patterson, A. Griffiths, Q. He, A. Yildiz, R. Mathies, *Rapid and fully microfluidic Ebola virus detection with CRISPR-Cas13a*, ACS Sensors 4 (4) (2019) 1048–1054.
[19] A. Bonini, N. Poma, F. Vivaldi, D. Biagini, D. Bottai, A. Tavanti, F. Di Francesco, *A label-free impedance biosensing assay based on CRISPR/Cas12a collateral activity for bacterial DNA detection*, J. Pharm. Biomed. Anal. 204 (2021) 114268.
[20] X. Cheng, Y. Li, J. Kou, D. Liao, W. Zhang, L. Yin, S. Man, L. Ma, *Novel non-nucleic acid targets detection strategies based on CRISPR/Cas toolboxes: A review*, Biosens. Bioelectron. 215 (2022) 114559.
[21] Z. Mao, X. Wang, R. Chen, Z. Zhou, S. Ren, J. Liang, Z. Gao, *Upconversion-mediated CRISPR-Cas12a biosensing for sensitive detection of ochratoxin A*, Talanta 242 (2022) 123232.
[22] Abnous, K., A. khakshour Abdolabadi, M. Ramezani, M. Alibolandi, M.A. Nameghi, T. Zavvar, Z. Khoshbin, P. Lavaee, S.M. Taghdisi, and N.M. Danesh, *A highly sensitive electrochemical aptasensor for cocaine detection based on CRISPR-Cas12a and terminal deoxynucleotidyl transferase as signal amplifiers.* Talanta, 2022: p. 123276.
[23] J. Wen, H. Deng, D. He, Y. Yuan, *Dual-functional DNAzyme powered CRISPR-Cas12a sensor for ultrasensitive and high-throughput detection of Pb2+ in freshwater*, Sci. Total Environ. 911 (2024) 168708.
[24] Z. Ji, Z. Shang, M. Sohail, P. Wang, B. Li, X. Zhang, G. Chen, *A CRISPR-enabled fluorometric biosensor for the sensitive detection of heparin antidote protamine based on programmable nuclease Cas12a*, Sens. Actuators B 374 (2023) 132709.
[25] Y. Zhao, L. Zhu, Y. Ding, W. Ji, K. Liu, K. Liu, B. Gao, X. Tao, Y.-G. Dong, F.-Q. Wang, *Simple and cheap CRISPR/Cas12a biosensor based on plug-and-play of DNA aptamers for the detection of endocrine-disrupting compounds*, Talanta 263 (2023) 124761.
[26] L. Peng, J. Zhou, G. Liu, L. Yin, S. Ren, S. Man, L. Ma, *CRISPR-Cas12a based aptasensor for sensitive and selective ATP detection*, Sens. Actuators B 320 (2020) 128164.
[27] J. Wang, X. Yang, X. Wang, W. Wang, *Recent advances in CRISPR/Cas-Based biosensors for protein detection*, Bioengineering 9 (10) (2022) 512.
[28] J. Shen, X. Zhou, Y. Shan, H. Yue, R. Huang, J. Hu, D. Xing, *Sensitive detection of a bacterial pathogen using allosteric probe-initiated catalysis and CRISPR-Cas13a amplification reaction*, Nat. Commun. 11 (1) (2020) 267.
[29] Z. Lv, Q. Wang, M. Yang, *Multivalent duplexed-aptamer networks regulated a CRISPR-Cas12a system for circulating tumor cell detection*, Anal. Chem. 93 (38) (2021) 12921–12929.
[30] F. Zhu, Q. Zhao, *CRISPR/Cas12a linked sandwich aptamer assay for sensitive detection of thrombin*, Anal. Chim. Acta 1287 (2024) 342106.
[31] R. Yang, L. Zhao, X. Wang, W. Kong, Y. Luan, *Recent progress in aptamer and CRISPR-Cas12a based systems for non-nucleic target detection*, Crit. Rev. Anal. Chem. (2023) 1–18.

[32] N. Liu, R. Liu, J. Zhang, *CRISPR-Cas12a-mediated label-free electrochemical aptamer-based sensor for SARS-CoV-2 antigen detection*, Bioelectrochemistry 146 (2022) 108105.
[33] C. Han, W. Li, Q. Li, W. Xing, H. Luo, H. Ji, X. Fang, Z. Luo, L. Zhang, *CRISPR/Cas12a-Derived electrochemical aptasensor for ultrasensitive detection of COVID-19 nucleocapsid protein*, Biosens. Bioelectron. (2021) 113922.
[34] L. Qi, J. Liu, S. Liu, Y. Liu, Y. Xiao, Z. Zhang, W. Zhou, Y. Jiang, X. Fang, *Ultrasensitive Point-of-Care Detection of Protein Markers Using an Aptamer-CRISPR/Cas12a-Regulated Liquid Crystal Sensor (ALICS)*, Anal. Chem. 96 (2) (2024) 866–875.
[35] S. Menon, M.R. Mathew, S. Sam, K. Keerthi, K.G. Kumar, *Recent advances and challenges in electrochemical biosensors for emerging and re-emerging infectious diseases*, J. Electroanal. Chem. 878 (2020) 114596.
[36] Y. Li, R. He, Y. Niu, F. Li, *Based Electrochemical Biosensors for Point-of-Care Testing of Neurotransmitters*, Journal of Analysis and Testing 3 (1) (2019) 19–36.
[37] O. Surucu, E. Öztürk, F. Kuralay, *Nucleic Acid Integrated Technologies for Electrochemical Point-of-Care Diagnostics: A Comprehensive Review*, Electroanalysis 34 (2) (2022) 148–160.
[38] M.S. Alam, *Proximity ligation assay (PLA)*, Curr. Protoc. Immunol. 123 (1) (2018) e58.
[39] A. Blokzijl, R. Nong, S. Darmanis, E. Hertz, U. Landegren, M. Kamali-Moghaddam, *Protein biomarker validation via proximity ligation assays*, Biochimica et Biophysica Acta (BBA)-Proteins and Proteomics 1844 (5) (2014) 933–939.
[40] H. Lv, J. Wang, J. Zhang, Y. Chen, L. Yin, D. Jin, D. Gu, H. Zhao, Y. Xu, J. Wang, *Definition of CRISPR Cas12a T rans-cleavage units to facilitate CRISPR diagnostics*, Front. Microbiol. 12 (2021) 766464.
[41] Y. Dai, R.A. Somoza, L. Wang, J.F. Welter, Y. Li, A.I. Caplan, C.C. Liu, *Exploring the trans-cleavage activity of CRISPR-Cas12a (cpf1) for the development of a universal electrochemical biosensor*, Angew. Chem. 131 (48) (2019) 17560–17566.
[42] Y. Lo, Y.-W. Cheung, L. Wang, M. Lee, G. Figueroa-Miranda, S. Liang, D. Mayer, J. A. Tanner, *An electrochemical aptamer-based biosensor targeting Plasmodium falciparum histidine-rich protein II for malaria diagnosis*, Biosens. Bioelectron. 192 (2021) 113472.
[43] L. Zhang, X. Fang, X. Liu, H. Ou, H. Zhang, J. Wang, Q. Li, H. Cheng, W. Zhang, Z. Luo, *Discovery of sandwich type COVID-19 nucleocapsid protein DNA aptamers*, Chem. Commun. 56 (70) (2020) 10235–10238.
[44] D. Zhang, Y. Yan, H. Que, T. Yang, X. Cheng, S. Ding, X. Zhang, W. Cheng, *CRISPR/Cas12a-Mediated interfacial cleaving of hairpin DNA reporter for electrochemical nucleic acid sensing*, ACS Sensors 5 (2) (2020) 557–562.
[45] L. Manning, M. Laman, D. Stanisic, A. Rosanas-Urgell, C. Bona, D. Teine, P. Siba, I. Mueller, T.M. Davis, *Plasma Plasmodium falciparum histidine-rich protein-2 concentrations do not reflect severity of malaria in Papua new guinean children*, Clin. Infect. Dis. 52 (4) (2011) 440–446.
[46] Pollock, N.R., T.J. Savage, H. Wardell, R.A. Lee, A. Mathew, M. Stengelin, and G.B. Sigal, Correlation of SARS-CoV-2 nucleocapsid antigen and RNA concentrations in nasopharyngeal samples from children and adults using an ultrasensitive and quantitative antigen assay. Journal of clinical microbiology, 2021. **59**(4): p. e03077-20.
[47] L.T. Nguyen, B.M. Smith, P.K. Jain, *Enhancement of trans-cleavage activity of Cas12a with engineered crRNA enables amplified nucleic acid detection*, Nat. Commun. 11 (1) (2020) 4906.